Available online at www.sciencedirect.com
ScienceDirect
Acta Materialia 57 (2009) 4866–4873
Acta MATERIALIA
www.elsevier.com/locate/actamat

Stick–slip dynamics of coherent twin boundaries in copper

Qiyang Hu [a], Lan Li [b], N.M. Ghoniem [a,*]

[a] Mechanical and Aerospace Engineering, University of California, Los Angeles, CA 90095, USA
[b] Microsoft Corporation,1 Microsoft Way, Redmond, WA 98052, USA

Received 9 June 2009; received in revised form 28 June 2009; accepted 28 June 2009
Available online 29 July 2009

Abstract

The migration kinetics of coherent twin boundaries (CTBs) and the underlying atomistic mechanisms are determined through molecular dynamics (MD) computer simulations. Details of motion dynamics and associated effective migration of CTBs are examined for nanotwinned copper crystals under externally applied shear loading. The present study reveals that the magnitude and direction of the resulting CTB migration velocity is dependent on the shear-loading orientation. It is found that $\langle 1\,1\,2\rangle$-type shearing on $\{1\,1\,1\}$ twin boundaries maximizes their transverse migration velocity. Shearing at directions which remain parallel the TB plane but are inclined to the $\langle 1\,1\,2\rangle$-direction results in a smaller degree of coupling, and finally to twin boundary sliding alone when the shear direction is along $\langle 1\,1\,0\rangle$. It is found that the dynamics of CTB motion can be described as a two-step "stick–slip" process. Analysis of atomic configurations indicates that the "stick" phase of the dynamics is associated with accumulated strain in the crystal, and that such strain is suddenly released by the nucleation of 1/6 $[1\,1\,2]$-type twinning partial dislocations. In atomic layers adjacent to the twin boundary, coordinated shuffling of atoms is found to take place immediately before dislocation nucleation. The "slip" phase of the dynamics is shown to be controlled by fast propagation of nucleated twinning partial dislocations and their spreading along the twin boundary.

Keywords: Copper; Interface migration; MD simulations; Twinning; Twin boundary

1. Introduction

The motion of grain boundaries (GBs) in response to applied external forces has been the subject of investigation for the last few decades, mainly because of the direct relationship between GB motion and macroscopic mechanical properties. It has been realized for some time that atomic-level mechanisms are in fact responsible for GB motion, and that there are strong correlations between GB structures and their ability to move under applied stress. Ashby outlined atomistic aspects of GB sliding in relationship to diffusional creep [1], and concluded that in order to accommodate creep deformation, GB sliding motion must be associated with other types of GB displacement modes. GB sliding results in incompatibilities, which must be accommodated either elastically through the deformation of neighboring grains, or plastically through the motion of dislocations [1]. More recently, Cahn and Taylor proposed a unified approach to the motion of GBs, where GB sliding is a special case of motion, and that in general, the relative tangential motion of two adjacent grains is associated with a proportional motion normal to the GB itself [2–4]. Moreover, the relative translation of two adjacent grains must also involve grain rotations [3,4]. Utilizing molecular dynamics (MD) simulations over the entire misorientation range and a wide range of temperatures, Cahn et al. determined the coupling factor between the tangential and normal motion for a $[0\,0\,1]$ symmetrical tilt GB in copper [4]. They also found the coupling factor β, defined as the ratio of normal-to-tangential velocities, to be multi-valued, and that it can be positive or negative. A simplified geometric model of coupling was proposed on the basis of crystal symmetry by Cahn et al., and was found to be in good agreement with MD simulations [4].

* Corresponding author. Tel.: +1 310 825 4866; fax: +1 310 206 4830.
E-mail address: ghoniem@ucla.edu (N.M. Ghoniem).

1359-6454/$36.00
doi:10.1016/j.actamat.2009.06.051

There are four modes of GB motion: (i) motion normal to the boundary, (ii) coupled tangential/normal motion, (iii) rigid-body GB sliding, and (iv) GB rotation [4]. Several experimental studies have explored these modes of twin boundary motion, especially the coupled tangential/normal motion under applied stress. Kizuka et al. observed that shearing of nanometer-sized gold contacts results in coherent twin boundary (CTB) coupled motion [5]. Using channel die deformation and imaging, Field et al. experimentally observed CTB migration in copper during severe deformation [6] and concluded that twin boundaries are sources of dislocations. Detailed experimental observations of twin boundary migration via twinning partial dislocation emission from twin boundary/GB intersections were provided by Wang et al. in their investigation of nanotwinned copper [7]. More recently, Molodov et al. performed an experimental investigation on the migration of low-angle tilt GBs in Al bicrystals [8]. The measured values of β were found to be in very good agreement with the Cahn et al. model [4]. In a similar experimental study, Winning performed in situ observations of coupled GB motion in Al bicrystals with $\langle 1\,1\,2\rangle$- and $\langle 1\,0\,0\rangle$-symmetric tilt boundaries with X-ray diffraction [9,10]. They inferred from their study that the migration mechanisms are the same for the coupled motion as for pure boundary migration, and that the primary mechanism is GB dislocation climb.

The coupled tangential/normal motion of GBs has been the subject of recent theoretical interest in order to uncover the conditions and generality of such motion, and to ascertain the nature of dynamics taking place. MD simulations were carried out by Zhang et al. on a Ni bicrystal for both low Σ and general [0 1 0] tilt boundaries [11]. These computer simulations revealed two critical stresses: one for coupled shear/boundary motion and the other for GB sliding, and for general tilt boundaries, the critical stress for coupled shear/boundary motion was found to be smaller than that for sliding. While the atomic structure and modes of GB motion have been investigated in detail in recent years, few studies have focused on the atomistic mechanisms and ensuing collective dynamics of GBs under external stress. The atomic motion within stationary and migrating asymmetric tilt GBs has been revealed by MD simulations, coupled with atomic trajectory analysis methods by Zhang et al. [12]. Two types of dynamic events within GBs were found: a string-like cooperative motion parallel to the tilt axis, and atomic motion across the GB plane occurring on a longer characteristic timescale of ~150 ps [12]. Dynamic analysis of GB motion using MD simulations indicated that, at low velocities, reversals of GB displacements were observed, indicating the presence of a crossover between the stick–slip and driven Brownian regimes [13].

The objective of the present work is to investigate the atomistic mechanisms responsible for the migration of symmetric $\Sigma 3$ CTBs. In our recent related work, we investigated the structure and motion of junctions between coherent and incoherent twin boundaries in copper [14], and the competition between dislocation and twin boundary motion in determining twin size effects on the deformation of nanotwinned copper [15]. In the present work, MD simulations of the shearing of isolated $\Sigma 3$ CTBs will be performed for a variety of shearing directions parallel to the plane of the GB in order to understand how CTBs migrate in response to an applied stress field. The atomic mechanisms responsible for the coupled motion along the shear direction and normal to the twin boundary plane [2–4] will be discussed. Those mechanisms will be further elucidated to ascertain the origins of an observed z"stick–slip" motion that controls the boundary migration rate. We will present an analysis of the stick–slip process to show that twinning partial dislocation nucleation is the initiating event responsible for twin boundary migration. Following a brief description of the computational procedure and numerical methods in Section 2, the results of MD simulations of an isolated CTB will be explored in Section 3. The atomic mechanisms responsible for the coupled motion along the shear direction and normal to the twin boundary plane will also be discussed. In Section 4, detailed analysis of the atomistic mechanisms responsible for CTB migration will be presented to ascertain the origins of the stick–slip process that controls the boundary migration rate. Finally, a summary of the present work and conclusions are given in Section 5.

2. Computer simulation procedures

Atomic interactions in Cu are modeled here using an accurate embedded-atom method (EAM) potential constructed by fitting to experimental and first-principles data [16]. MD simulations were performed using two different codes: LAMMPS [17] and XMD [18]. A methodology similar to that described by Cahn et al. [4] was followed in order to simulate the shearing of an isolated boundary. The chosen $\Sigma 3$ GBs were initially created by standard geometric constructions of the coincidence site lattice (CSL) model [19]. MD simulations were performed in the canonical (NVT) ensemble, using a constant-temperature Nose–Hoover-type thermostat. Prior to beginning an MD simulation, the computational block was subjected to a uniform expansion corresponding to the the chosen temperature. This a priori process takes into account the thermal expansion that would take place naturally, and so maintains the simulation block at zero average pressure. The thermal expansion factors were determined by Mishin et al. [16] using zero-pressure Monte Carlo simulations. As shown in Fig. 1, fixed boundaries were imposed in the z-direction by creating thin slabs of fixed atoms at the top and bottom of the simulation block. These thin slabs were allowed to interact with their neighbors, but the atoms in the thin slabs were moved as a single unit. By applying a constant velocity to the upper fixed region while holding the lower region motionless, an external shear stress parallel to the GB was introduced. The statistics of defects and twin boundaries are recorded utilizing the central symmetry method [20].

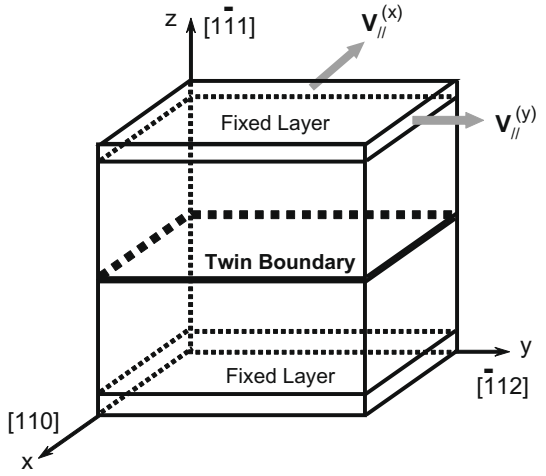

Fig. 1. Twin boundary shear simulation block geometry used in this paper. The areas labeled "Fixed Layer" indicate a layer of atoms which remain fixed relative to each other and move as a rigid-body. Periodic boundary conditions are imposed in the x ([1 1 0]) direction. Simulations were performed with y ([$\bar{1}$ 1 2]) planes periodic in Section 3, and free surfaces in Section 4. $v_{\parallel}^{(x)}$ and $v_{\parallel}^{(y)}$ are the velocity components along x and y directions applied to the upper fixed slab.

To investigate the detailed mechanisms of twin boundary migration, we set up a simulation box as follows. The x, y and z axes of the simulation cell were selected as [1 1 0], [$\bar{1}$ 1 2], and [1 $\bar{1}$ 1], respectively, with twin interfaces on x–y planes (1 $\bar{1}$ 1) (see Fig. 1). The simulation box is 20 nm along all the x, y and z directions, and consists of 0.5 million atoms, and uniform shear strains on the (1 $\bar{1}$ 1)-plane were applied.

3. Stick–slip dynamics

Stick–slip motion is generally associated with the sliding of two contacting surfaces or the peeling of soft matter off of a hard surface. Nonlinear dynamical models show that the resulting motion is jerky, and leads to well-known instabilities. However, the physical details of the mechanisms responsible for such motion are system dependent. Recently, Mishin et al. demonstrated a close relationship between coupled GB motion in crystals and other cases of stick–slip dynamics by applying accelerated MD simulations [13].

The standard simulation case here is set up with a uniform shear strain rate of 1.5×10^9 s^{-1}, along the [$\bar{1}$ 1 2] direction at a temperature of 200 K. In these simulations, we applied periodic boundary conditions along both the x ([1 1 0]) and y ([$\bar{1}$ 1 2]) directions. The simulations reveal that the transverse migration of a coherent twin boundary can also be regarded as a stick–slip process. Initially the system stays in an inertial stick stage, followed by a slip process that occurs suddenly, resulting in boundary migration normal to its plane over a distance of one atomic layer. This process is observed to be repetitive, though not exactly periodic. Thus the nominal migration velocity of a twin boundary is an average result of both the transient slip speed and the stick incubation time. To determine average (effective) migration speeds of twin boundaries, we utilize least-square statistics on multiple slip and stick processes. The average slope of the transverse displacement vs. elapsed time gives the equivalent transverse twin migration velocity, while the standard error would provide information on the physical nature of the stick–slip process. Larger fluctuations in the displacement–time relationship indicate that twin boundary migration is highly discontinuous, with obvious stick–slip motion, while lower values denote less significant influence of the stick stage of motion.

The migration profile of the CTB is shown as a thick dark line in Fig. 2. A coupling constant, β, for the boundary was introduced by Cahn et al. as the ratio of the CTB migration velocity (transverse) to the grain translation (slip) velocity [3]. The present simulations indicate that $\beta = \frac{v_t}{v_s} \approx 0.81 \pm 0.009$. This result is consistent with the displacement shift complete (DSC) theory [19], in which the ratio of transverse to sliding speed is calculated as $\beta_0 = (a/6[\bar{1}\,1\,2]_I)/(a/3[1\,\bar{1}\,1]_I) = 1/\sqrt{2} \approx 0.71$. An important finding from our MD simulations is that the magnitude and direction of the CTB migration speed are strongly influenced by the direction of the shear stress on {1 $\bar{1}$ 1}-planes. We selected four different directions on the (1 $\bar{1}$ 1) plane, denoted by (*a*), (*b*), (*c*) and (*d*). Direction (*a*) is [$\bar{1}$ 1 2], (*d*) is [1 1 0], (*b*) is 15° clockwise to [$\bar{1}$ 1 2] and (*c*) is 45° counterclockwise to [1 1 0].

As shown in Fig. 2, the downward maximum speed of the CTB migration occurs along the direction of [$\bar{1}$ 1 2] and every 120° to [$\bar{1}$ 1 2] on {1 $\bar{1}$ 1} planes. If the shear is along the [1 1 0]-directions, no CTB migration is observed.

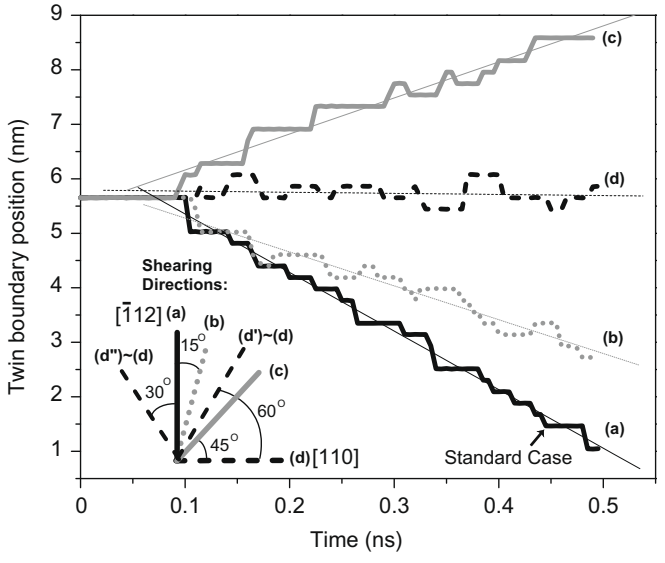

Fig. 2. Dependence of CTB transverse displacement on the direction of shear loading on the {1 1 1} plane at a strain rate of 1.5×10^9 s^{-1} and 200 K. Thick lines are MD simulation results, while thin lines are linear fits to simulations. Four different directions on {1 1 1}-planes are denoted by (a–d), as shown in the inset. Directions (*d'*) and (*d''*) have a statistically equivalent motion as the (d) direction.

For every 60°, the CTB would change the migration up–down direction. This relationship can be illustrated more clearly in Fig. 3, where different colors (white, light grey, dark grey) denote atoms on three consecutive {1 1 1}-planes. The maximum absolute value of positive migration velocity is reached for off 30° to [1 1 0], while the maximum absolute value of the negative migration velocity is reached at 90° to [1 1 0], as shown in the figure. Since CTB migration induced by (1 1 1) shearing strain exhibits a 3-fold symmetry in an face-centered cubic (fcc) crystal lattice, the coupling constant is thus a function of $\sin(3\theta)$, where θ is the angle of the shear direction relative to [1 1 0] on $(1\bar{1}1)$-planes. The simulation results for the coupling constant, β, are given in Table 1. Note that coupled motion in response to shear in [1 1 0] is prohibited by symmetry, since $\theta = 0$.

Further investigations indicated that while the details of GB migration are time dependent and show stochastic behavior, the overall average velocity is essentially controlled by the crystal geometry and shearing direction. At a shearing angle of 90° to the [1 1 0]-direction, Fig. 4 shows the twin boundary displacement vs. the top layer displacement during shear loading at 200 K, in which it is clear that

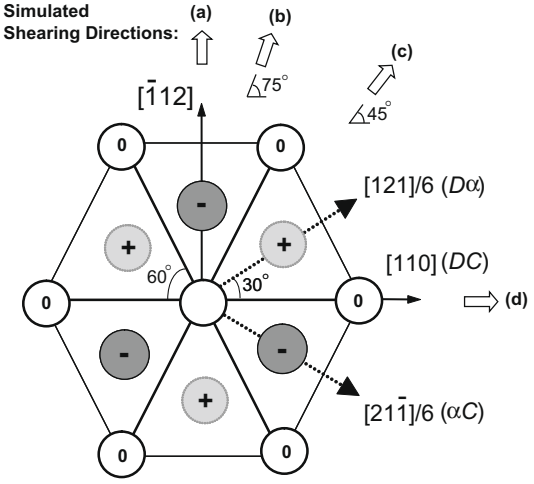

Fig. 3. Illustration of crystal geometry on $(1\bar{1}1)$-plane under various shear loadings with different directions denoted by block arrows (a–d). Dotted lines with arrows denote two possible twinning parital directions which correspond to $D\alpha$ and αC in the Thompson tetrahedron. "0" denotes base middle layer atoms, while "+" and "-" denote upper and lower layer atoms, respectively. $D\alpha$ partials result in the moving-up CTB migration with the maximum velocity; αC result in the moving-down CTB migration with the maximum velocity. Full dislocation DC statistically results in no migration of CTBs due to the cancellation effect of the vertical migrations of CTBs from $D\alpha$ and αC.

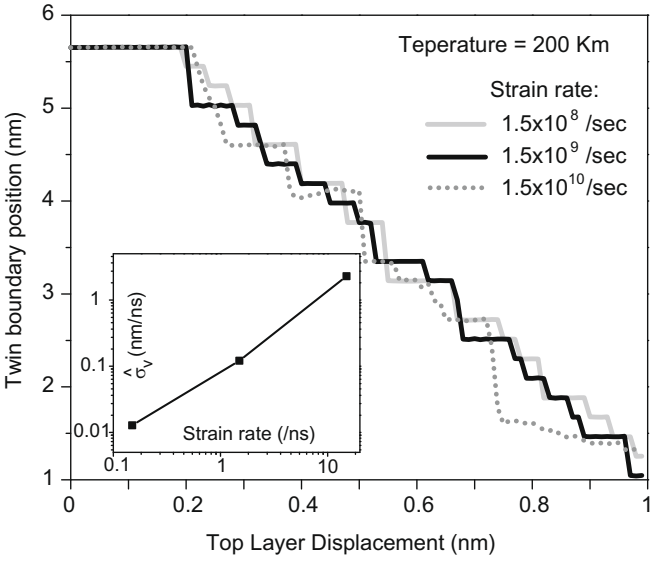

Fig. 4. Twin boundary position plotted as a function of total shear displacement of the upper fixed region. The shear direction is at 75° from the [1 1 0]-direction.

the migration velocity is proportional to the slip velocity resulting in β being constant. The fluctuation in the migration velocity ($\hat{\sigma}_v$), which can be regarded as a measure of the driven Brownian component of the dynamics [13], is found to increase with the strain rate. Our statistical analysis shows that the equivalent migration velocity is 10.745 ± 0.121 m s^{-1}, where 0.121 m s^{-1} is the standard deviation in the boundary velocity ($\hat{\sigma}_v$), shown in the figure inset. It is interesting to note here that the higher the strain rate, the faster the TB migration speed, and the more distinct is the stick–slip nature of the motion. For example, the gray dotted line in Fig. 4 clearly shows a much longer stick stage and a more distinct slip displacement.

The temperature is found not to influence twin boundary migration, as can be seen in Fig. 5, where the migration velocity is about 10.7 m s^{-1} in the range of 200–600 K. However, the displacement steps become smaller as the temperature is increased. This is not very surprising, since thermal fluctuations tend to smooth out the discontinuous stick–slip process. These observations are consistent with the recent analysis of the transition from stick–slip to driven Brownian dynamics of stressed GBs, proposed by Mishin et al. [13].

4. Atomistic mechanism for stick–slip CTB migration

To reveal the atomistic origins of CTB motion and the influence of crystal free surfaces, MD simulations were

Table 1
Statistical analysis results and comparisons of CTB migrations at different shear directions to [1 1 0].

Angle θ to [1 1 0]	90°	75°	0°	45°
v_t (m/sec)	-10.745 ± 0.121	-6.214 ± 0.173	-0.2 ± 0.157	6.616 ± 0.159
$\beta = v_t/v_s$	-0.81 ± 0.009	-0.468 ± 0.013	-0.015 ± 0.012	0.5 ± 0.012
$\beta_0 \cdot \sin(3\theta)$	-0.71	-0.5	0	0.5

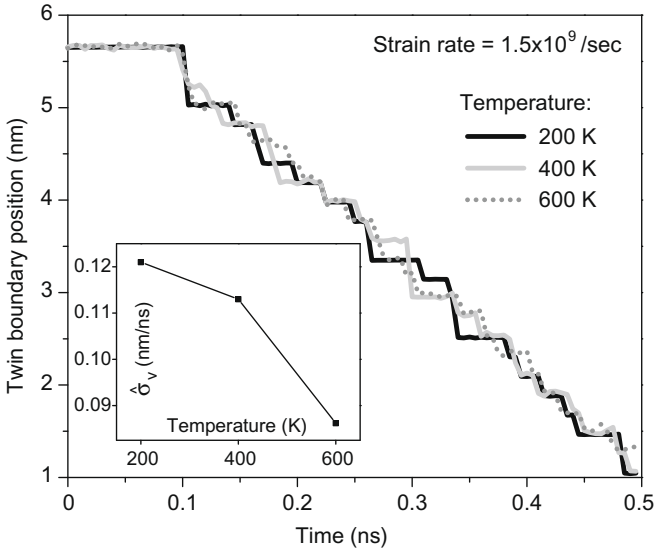

Fig. 5. Twin boundary position plotted as a function of time for several temperatures under a constant strain rate of $1.5 \times 10^9\ s^{-1}$. The shear is along $[\bar{1}\,1\,2]$. The coupled motion of the CTB is shown to be relatively independent of temperature.

performed with the bounding $(\bar{1}\,1\,2)$ planes in Fig. 1 taken as free crystal surfaces, while the x-direction has still periodic boundary conditions. Simulations were performed in two stages: first, the system is elastically preloaded up to 6.9% uniform shear strain, and then constant strain rates in the range 5×10^7–$5 \times 10^9\ s^{-1}$ were applied. While atoms in the bottom layer of the MD cell were fixed, the positions of atoms in the top layer were constrained to those obtained from simple shear displacements. MD simulations of all atoms within the cell in response to the prescribed displacement were conducted at a temperature of 300 K.

The stick–slip mechanism is found to be essentially a two-step process, where the "stick" phase is associated with the accumulation of significant strain throughout the crystal, and is terminated by strain localization near the CTB, leading to the nucleation of twinning partial dislocations. This first phase is relatively long, lasting on the order of 20–50 ps, and is mainly dependent on the applied strain rate. The second phase proceeds at a timescale that is 1–2 orders of magnitude smaller, and is mediated by the rapid expansion of nucleated twinning partial dislocations across the twin boundary interface. Fig. 6 shows a time sequence of the process of twin boundary migration as a result of the nucleation and spreading of a twinning partial dislocation loop, initiated at the intersection of the twin boundary with the two opposing surfaces of the simulation cell. The white atoms are those with the number of nearest neighbors different from 12, indicating departure from equilibrium positions associated with severe lattice distortions or transient atomic "shuffling". The red atomic plane is the original twin interface, while the green atomic plane is the new twin interface, after the original interface translated by one atomic layer. We can clearly see several stages of the twin boundary migration mechanism illustrated in Fig. 6. The twin boundary is shown before migration in (a) at 0.2 ps. Clusters of shuffled atoms are first nucleated close to the left side surface and move towards the right side in a coherent motion, as shown in (b) and (c) at 1–1.8 ps. At 4.6 ps, the coherent group of shuffled atoms moves along the $(1\,\bar{1}\,1)$ plane, and then disassociates on the front and back surfaces, as shown in (d). The motion of this wave of shuffled atoms localizes the strain and results in the nucleation of a twinning partial loop (two half-loops because of the periodic boundary) at 5.6 ps. At 7.8 ps, the two twinning partial dislocations slip over the $(1\,\bar{1}\,1)$ plane adjacent to the twin boundary leading to transverse translation of the twin boundary one atomic step, as seen in (f). The two curved partial dislocations then merge in the middle of the cell at 8.4 ps in (g), and at 9 ps, a new partial dislocation loop nucleates homogeneously at the merging point, spreading outwards, followed by the formation of a second twin boundary that is one layer above the first one. We examined the distorted lattice structure and the Burgers circuit for the white atoms, and found that, except for the ones adjacent to the new twin boundary (green atoms), the white atoms are in regions with closed Burgers circuits with no net Burgers vector. This indicates that the atoms showing coherent group motion do not actually form dislocations, and that they are shuffled atomic clusters on atomic layers adjacent to the twin boundary plane.

In order to better understand the nature of shuffled atoms that are precursors to twinning partial dislocation nucleation, we performed a Burgers circuit analysis across the twin boundary interface. Fig. 7 shows the Burgers circuit to identify the partial dislocation along the twin boundary interface, leading to step generation (a twinning dislocation), consistent with the schematic discussed in Ref. [21]. In Fig. 7, white atoms are in perfect lattice positions, blue atoms mark the twin boundary, yellow atoms delineate the dislocation core, and the two small yellow arrows indicate the position of the new twin plane. The Burgers circuit construction in Fig. 7 clearly shows that the closure failure vector is $\frac{1}{6}[1\,1\,2]$, and that the nucleated twinning partial dislocation has an edge character.

Fig. 8 shows a sketch that illustrates the twin boundary migration mechanism as a consequence of twinning partial nucleation and motion in an fcc crystal [21,22]. However, our current MD simulations clearly show the precursor conditions leading to twinning partial nucleation, and the detailed dynamics of motion that result in CTB migration. Suppose we have a twin boundary with layers ACB|A|BCA. If a partial dislocation glides over a $(1\,\bar{1}\,1)$-type plane adjacent to the twin boundary, it will move all lattice atoms in an area below its slip plane a distance equal to the magnitude of one Burgers vector. So the layer of atoms in B positions will be moved to a C position. Simultaneously, atoms in C positions will move to A positions, and those in an A position will move to a B position, etc. As the twinning partial glides over the twin boundary interface, all atoms in the lower part of the crystal will be moved according to the described sequence outlined here. Finally $(1\,\bar{1}\,1)$-type atomic planes

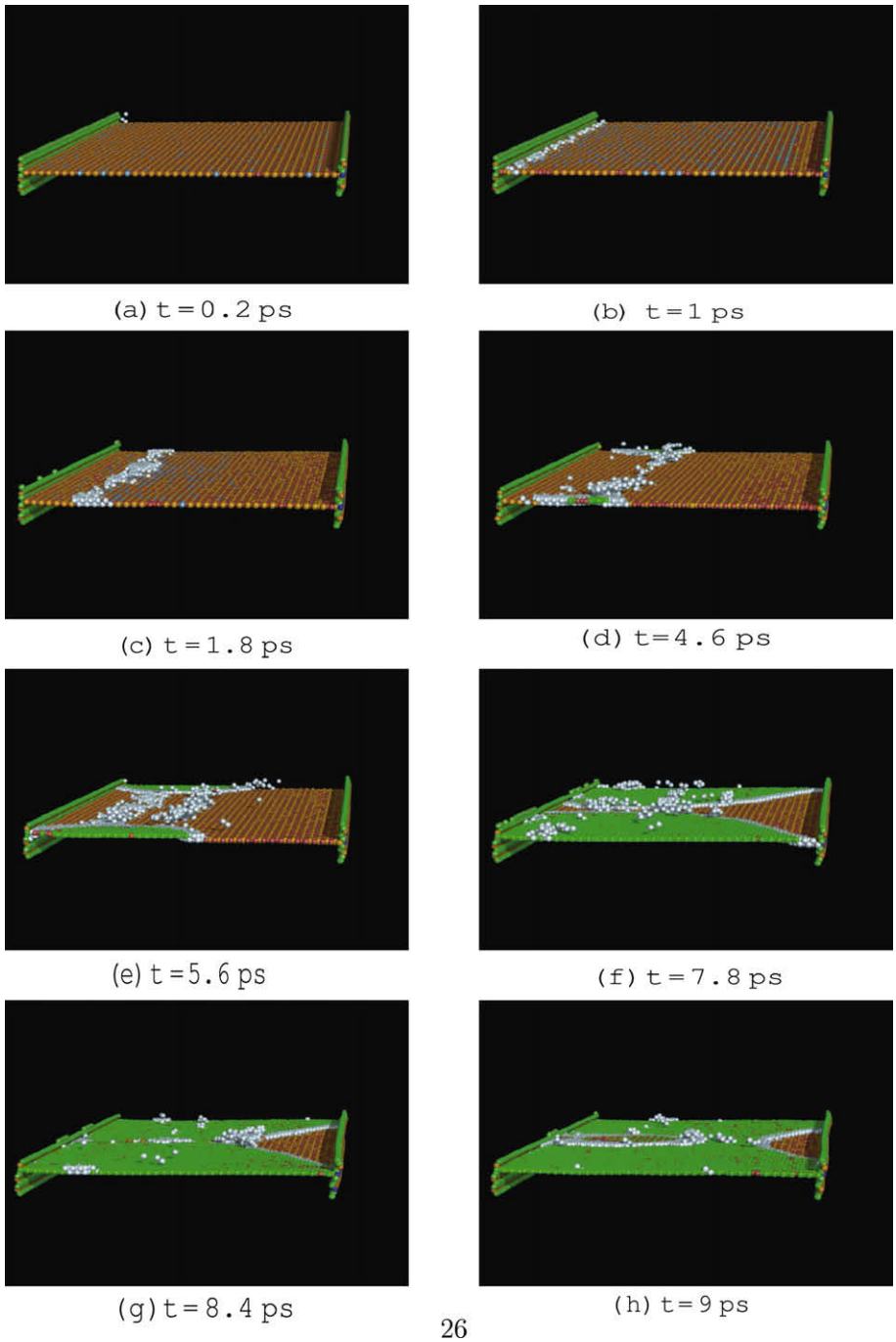

Fig. 6. Visualization of dislocation nucleation and motion on the twin boundary. The white atoms are in highly distorted positions (nearest neighbors different from 12). The red atomic plane is the original twin interface. The green atomic plane is the new twin interface which is one atomic layer above the red plane. The shear direction is along $[\bar{1}\,1\,2]$.

in the crystal lattice will have the sequence CBA|C|ABC, and thus the upper half of the lattice will still have the layout of ABC, while the lower half remains in the layout of CBA, but the twin interface has moved one layer downward and C is the new twin interface. While the mechanism of CTB migration is confirmed to be controlled by the nucleation and spreading of $\frac{1}{6}[1\,1\,2]$-twinning partial, its nucleation is induced by the coherent motion of shuffled atomic clusters in atomic layers adjacent to the CTB. Nucleation of twinning partials involved in the CTB migration mechanism is found not to be homogeneous, but is initiated at the layer directly adjacent to the twin boundary at the surface of the crystal. When two twinning partial dislocation loops with the same Burgers vector merge together in the middle of the twin plane, a new dislocation loop nucleates at the merging region, and on the plane adjacent to the newly formed twin boundary. Thus, the mechanism is repeatable with alternating nucleation sites of twinning partial loops between the

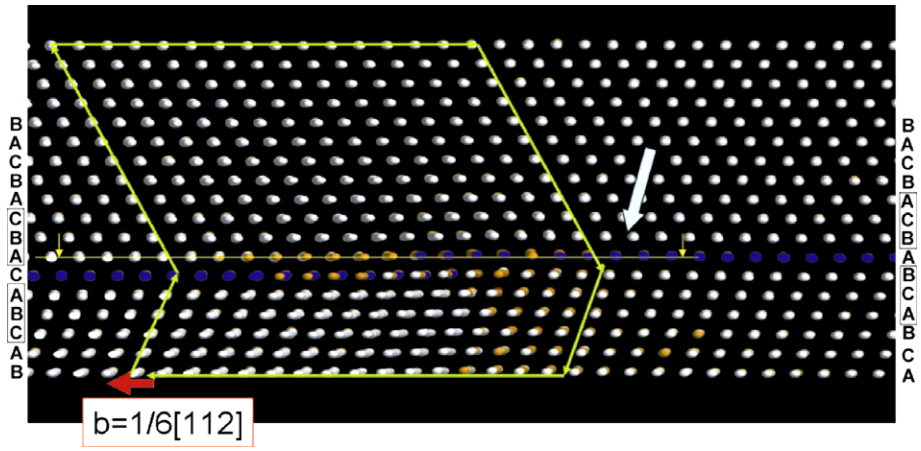

Fig. 7. Burgers circuit identifying a twinning partial dislocation (see text for details). Note that the white streaks represent rows of atoms, indicating a slight local lattice rotation, the yellow arrows delineate the position of the new twin plane, and the large white arrow shows the beginning of the new twin plane. The closed-packed layer sequences are illustrated on the graph.

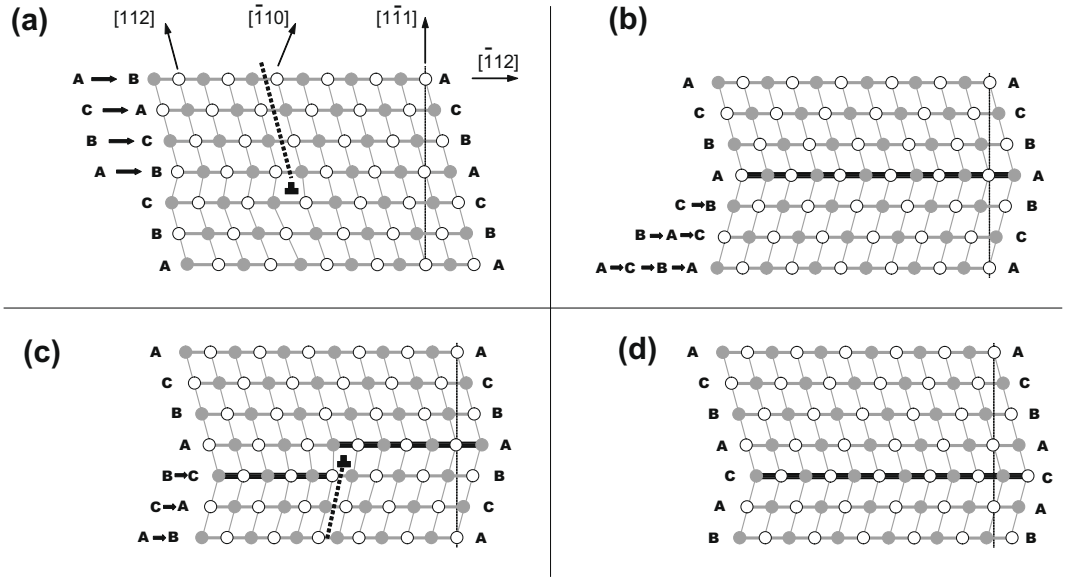

Fig. 8. Sketch of the twin boundary migration mechanism propagated by a twinning partial dislocation in an fcc crystal shown in the $\langle \bar{1}\,1\,0 \rangle$ projection plane. (a) The process of twin formation by successive twinning partial dislocations with intrinsic stacking faults; (b) completion of CTB formation as a result of continuous slips along close-packed layers; (c) lattice configuration during the CTB migration as a result of the propagation of a twinning partial; and (d) CTB migration competed.

crystal surfaces and its interior, and leads to the overall jerky motion of the twin boundary.

5. Discussion and conclusions

The present MD studies reveal that twin boundary migration can be described within the framework of stick–slip dynamics. Recently, Ivanov and Mishin have shown that coupled GB motion occurs by increments and can exhibit dynamics similar to the stick–slip behavior [23]. It is found that the initial stick phase is significantly longer than the period associated with the slip phase. While "stick" is controlled by the accumulation of localized strain to nucleate twinning partials, the "slip" phase corresponds to the spreading of nucleated twinning partial dislocations on the twin boundary interface. Another observation of the stick–slip dynamics is that the period associated with the stick stage gets shorter once the crystal is activated and once the twin boundary moves. Since the migration of twin boundaries corresponds to plastic deformation, the initial stick behavior can be considered as an accumulation of elastic strain energy. When the slip occurs, the system acquires kinetic energy due to released phonons, and inertial effects result in shortening of subsequent stick periods. It should be noted that during shear deformation, only one top layer is subjected to a constant displacement velocity externally, and no additional velocity gradients are imposed in the simulation block. In our simulations, we noticed that during the stick process

there exist significant energy fluctuations, which are found to be correlated with stacking sequence shuffling within the twin regions. The shuffling takes place in a transient way to achieve metastable equilibrium during the dynamics of stick–slip. The discrepancies between our simulated coupling constant β and the DSC β_0 may be attributed to this phenomena. In calculating the coupling constant β, we use a constant slip velocity imposed on the top layer, which in turn is transferred to the twin boundary interface through the crystal dynamics. As a result, the coupling constant is not purely geometric, as predicted by the DSC theory, but is somewhat dependent on the stick–slip dynamics. While the ratio of the tangential to normal speeds is dictated by crystal geometry, its instantaneous value is dependent on the CTB dynamics. Several twinning dislocations may be nucleated within a short duration. Thus, the normal translation of the CTB contains transient components that result in brief deviations from the geometric value. Another interesting phenomenon possibly related to the transient dynamic effect is the strengthened stick–slip motion during high-strain-rate loading conditions.

The stick stage of the dynamics is found to be controlled by twinning partial dislocation nucleation, induced by coordinated motion of shuffled atoms in a coherent "wave" that is initiated from the crystal surface. Nucleation of twinning partials involved in CTB migration mechanism is found to be heterogeneous adjacent to the twin boundary, at the surface of the crystal, and at stress concentration regions associated with shuffled atoms within the crystal. It is concluded that $\langle 1\,1\,2\rangle$-type shearing of the GB (along Shockley partial dislocation directions) maximizes the velocity of boundary migration, and that shearing at directions which remain parallel the GB plane but are inclined to the $\langle 1\,1\,2\rangle$-direction results in a smaller degree of coupling between tangential and transverse motion of CTBs.

Acknowledgements

This work is supported by the National Science Foundation Grant Nos. 0506841 and 0625299 with UCLA.

References

[1] Ashby M. Surf Sci 1972;31:498.
[2] Cahn JW, Mishin Y, Suzuki A. Philos Mag 2006;86:3965.
[3] Cahn JW, Taylor JE. Acta Mater 2004;52(16):4887.
[4] Cahn JW, Mishin Y, Suzuki A. Acta Mater 2006;54:4953.
[5] Kizuka T. Jpn J Appl Phys 2007;46(11):7396.
[6] Field DP, True BW, Lillo TM, Flinn JE. Mater Sci Eng A 2004;372:173.
[7] Wang YB, Sui ML, Ma E. Philos Mag Lett 2007;87(12):935.
[8] Molodov D, Ivanov V, Gottstein G. Acta Mater 2007;55:1843.
[9] Winning M. Philos Mag 2007;87(32):5017.
[10] Winning M. Scripta Mater 2008;58(2):85.
[11] Zhang H, Duy D, Srolovitz D. Philos Mag 2008;88(2):243.
[12] Zhang H, Srolovitz D, Douglas J, Warren J. Phys Rev B 2006; 74:115404.
[13] Mishin Y, Suzuki A, Uberuaga BP, Voter AF. Phys Rev B 2007;75:224101.
[14] Brown A, Ghoniem N. Acta Mater 2009;57(15):4454.
[15] Li L, Ghoniem N. Phys Rev B 2009;79(7):075444.
[16] Mishin Y, Mehl MJ, Papaconstantopoulos DA, Voter AF, Kress JD. Phys Rev B 2001;63:224106.
[17] Plimpton S, Crozier P, Thompson A; 2008. <http://lammps.sandia.gov/> .
[18] Rifkin, J; 2008. <http://xmd.sourceforge.net/>.
[19] Sutton AP, Balluffi RW. Interfaces in crystalline materials. Oxford: Clarendon Press; 1995.
[20] Kelchner CL, Plimpton SJ, Hamilton JC. Phys Rev B 1998; 58(17):11085.
[21] Boiko VS, Garber RIG, Kosevich AM. Reversible crystal plasticity. Springer; 1994.
[22] Hirth JP, Lothe J. Theory of dislocations. New York: John Wiley; 1982.
[23] Ivanov VA, Mishin Y. Phys Rev B 2008;78(6):064106.